Azolylborane Adducts. Structural and Conformational Analysis by X-ray Diffraction and NMR. Protic-Hydric ($C-H^{\delta+}\cdot\cdot\cdot{}^{\delta-}H-B$) and Protic-Fluoride ($C-H^{\delta+}\cdot\cdot\cdot{}^{\delta-}F-B$) Interactions

Itzia Irene Padilla-Martiñez*[a][+], Maria de Jesús Rosalez-Hoz[b], Hugo Tlahuext[c], Carlos Camacho-Camacho[d], Armando Ariza-Castolo[b], and Rosalinda Contreras*[b]

Departamento de Química, Unidad Profesional Interdisciplinaria de Biotecnología IPN[a],
Av. Acueducto S/N, Barrio la Laguna, Ticomán México, D.F. 07000 México

Departamento de Química, Centro de Investigación y de Estudios Avanzados del Instituto Politécnico Nacional[b],
A.P. 14-740, México, D.F. 07000 México

Facultad de Ciencias, Universidad Autónoma del Estado de Morelos[c],
Av. Univerdidad 1001 Col. Chamilpa, Cuernavaca Morelos, México

Departamento de Sistemas Biológicos, Universidad Autónoma Metropolitana Xochimilco[d],
Calzada del Hueso 1100, Col. Villa Quietud, México, 04960 México

Received October 31, 1995

Key Words: Azolylborane adducts / Boron–imidazole adducts / Boron–pyridine adducts / Protic-hydric interactions / Protic-fluoride interactions

The preparation, NMR and X-ray diffraction studies of a series of azolylboron hydrides derived from pyrrole, indole, and carbazole coordinated with tetrahydrofuran, pyridine, and imidazole are reported. The azolyl substituents are very electroattractive leading to an acidic boron atom which strongly coordinates with the Lewis bases. The stabilization of the $-BH_2-$ groups against disproportionation could be explained in terms of the interactions found between the acidic hydrogen atoms of the heterocycles ($C-H^{\delta+}$ acceptor) and the hydrides ($B-H^{\delta-}$ donors).

There are few examples of aminoboron hydrides NBH_2 derived from aromatic nitrogen heterocycles[1,2], in part because free XBH_2 boron dihydrides are not stable compounds, the XBH_2 group disproportionating to BH_3 and BX_3; however, the acidic boron atom of these compounds can be stabilized in a cycle by coordination as in the case of pyrazaboles[2c–d] and other XBH_2 compounds (X = O)[3]. It is relevant to understand the nature of the N–B bond[4] and the structural factors for stabilization of the $N-BH_2$ group which could include the donating ability of the nitrogen atoms, the ring aromaticity and the charge distribution. The (dialkylamino)boranes derived from pyrrole, indole, and carbazole were studied by ^{11}B-NMR spectroscopy[5,6].

Herein, the preparation and the study by NMR and X-ray diffraction analyses of a series of azolylboron hydrides derived from pyrrole, indole, and carbazole coordinated with tetrahydrofuran, pyridine, and imidazole is reported (Scheme 1). The imidazole–BF_3 adduct was also prepared in order to compare it with the azolylborane–imidazole adducts. We wanted to know the structural and electronic reasons for the stability of these boron compounds and how coordination affects their behaviour.

Scheme 1. Studied compounds with ring numbering

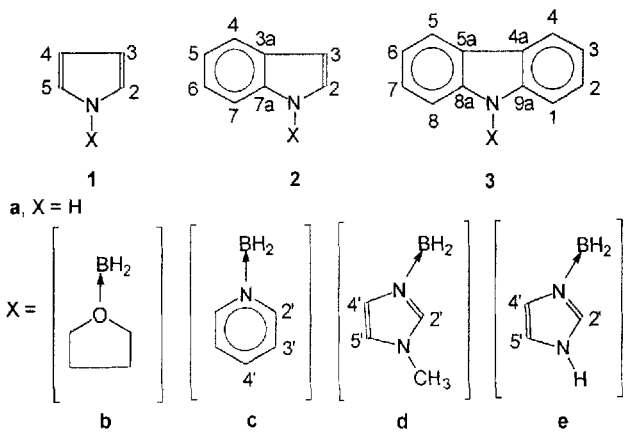

Results and Discussion

The azolylborane–THF complexes (Scheme 1) were synthesized from the equimolar reaction of the azole (**1–3**) and $BH_3 \cdot THF$. The reactions were followed by measuring the hydrogen evolution. When the reactions had finished the coordinating nitrogen heterocycles were added. The adducts were isolated by crystallization or precipitation from saturated THF solutions.

[+] This work is part of the I. I. Padilla-Martiñez PhD Thesis Cinvestav México, **1995**, and an abstract was presented at the 49th Southwest Regional Meeting of the American Chemical Society, Austin, Texas, October 24–27, **1993**.

  0009–2940/96/0404–0441 $ 15.00+.25/0

X-ray Diffraction Analysis of Azolylborane Adducts

The structures of the adducts pyrrolylborane–pyridine **1c**, pyrrolylborane–imidazole **1e**, indolylborane–*N*-methylimidazole **2d**, carbazolylborane–pyridine **3c**, and carbazolylborane–*N*-methylimidazole **3d** are shown in Figures 1–5.

Figure 1. Molecular structure of pyrrolylborane-pyridine **1c**. Bond lengths [pm] and bond angles [°]: N(1)-C(2) 132.5(5), N(1)-C(6) 134.4(4), N(1)-B(7) 161.9(5), N(8)-B(7) 152.2(6), N(8)-C(9) 136.8(5), N(8)-C(12) 135.4(6), C(10)-C(11) 138.5(7), B(7)-H(1A) 112(4), B(7)-H(1B) 110(5), C(2)N(1)C(6) 118.5(3), C(2)N(1)B(7) 120.9(3), C(6)N(1)B(7) 120.5(3), C(9)N(8)C(12) 106.6(4), C(9)N(8)B(7) 126.4(3), C(12)N(8)B(7) 127.0(3), C(9)C(10)C(11) 107.7(4), C(10)C(11)C(12) 106.4(5), N(1)B(7)N(8) 108.7(3), H(1A)B(7)H(1B) 116(3), N(2)C(2)C(3) 122(4), H(2)C(2)N(1) 115(4), H(6)C(6)N(1) 116(3), H(6)C(6)C(5) 123(2), H(9)C(9)N(8) 121(3), H(9)C(9)C(10) 130(4), H(12)C(12)N(8) 119(4), H(12)C(12)C(11) 130(3), H(1B)B(7)N(8)C(9) -14(3), H(1B)B(7)N(1)C(2) 36(3), H(1A)B(7)N(8)C(12) 33(2), H(1A)B(7)N(1)C(6) -22(2)

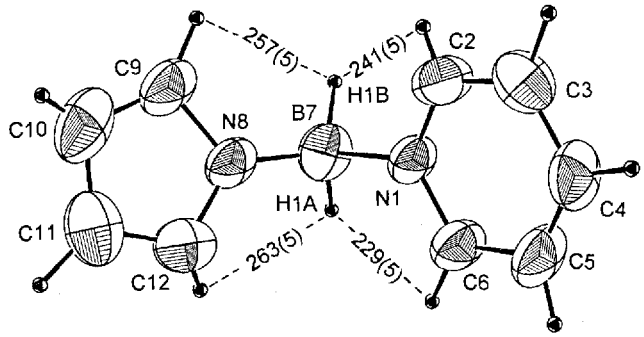

Figure 2. Molecular structure of pyrrolylborane-imidazole adduct **1e**. Bond lengths [pm] and bond angles [°]: N(1)-C(1) 133.6(3), N(1)-C(2) 133.1(3), N(2)-C(1) 131.6(3), N(2)-C(3) 134.6(3), C(2)-C(3) 130.7(3), C(5)-C(6) 136.4(4), B(1)-N(2) 157.5(4), B(1)-N(3) 151.4(4), B(1)-H(9) 109.0(4), B(1)-H(10) 112.0(3), N(2)B(1)N(3) 109.8(2), B(1)N(2)C(1) 126.6(3), B(1)N(2)C(3) 127.7(3), B(1)N(3)C(4) 127.8(3), B(1)N(3)C(7) 126.4(3), C(4)N(3)C(7) 105.7(2), C(1)N(2)C(3) 105.7(2), C(4)C(5)C(6) 108.1(3), C(5)C(6)C(7) 106.7(3), H(9)B(1)H(10) 113.0(3), H(1)C(1)N(2) 122.1(4), H(1)C(1)N(1) 128.9(4), H(3)C(3)N(2) 119.3(4), H(3)C(3)C(2) 130.2(4), H(4)C(4)N(3) 116.5(4), H(4)C(4)C(5) 133.6(5), H(7)C(7)N(3) 117.2(4), H(7)C(7)C(6) 133.1(5), H(9)B(1)N(3)C(7) -23.6(3), H(9)B(1)N(3)C(1) 33.3(3), H(10)B(1)N(3)C(4) 34.5(3), H(10)B(1)N(2)C(3) -29.2(3)

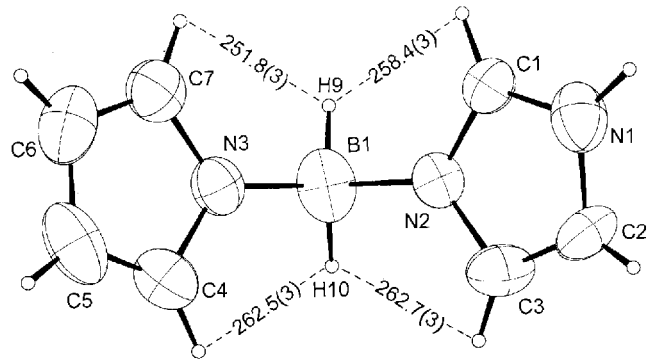

In all compounds the boron atom is tetrahedral and the covalent N–B bond distance is constant and shorter than the N→B-coordinated bond. The last one is significatively shorter for imidazole complexes (**1e**, **2d**, and **3d**) than for pyridine derivatives (**1c**, **3c**, Table 1). This result is an indication that the N→B bond in imidazoles is stronger than in pyridines.

The geometric changes in the azole ring of azolylborane adducts are in agreement with a higher electronic delocalization than in the free azole as observed by ^{13}C NMR spectroscopy (vide infra). In all azolyl rings the C–C bond

Figure 3. Molecular structure of indolylborane-N-methyl-imidazole adduct **2d**. Bond lengths [pm] and bond angles [°]: N(1)-B 150.3(6), C(7)-C(8) 141.9(7), N(10)-C(14) 130.1(5), N(10)-B 158.0(7), N(10)-C(11) 135.7(6), C(11)-C(12) 132.0(8), N(13)-C(12) 135.4(7), N(13)-C(14) 132.0(6), B-(H1A) 116(5), B-(H1B) 107(4), C(2)N(1)C(9) 104.6(3), C(2)N(1)B 127.5(4), C(9)N(1)B 127.8(4), C(2)C(7)C(8) 105.3(4), C(7)C(8)C(9) 107.3(4), C(11)N(10)C(14) 106.2(4), C(11)N(10)B 126.2(4), C(14)N(10)B 127.4(4), C(12)N(13)C(14) 106.3(4), N(10)C(11)C(12) 108.5(5), N(13)C(12)C(11) 107.7(5), N(10)C(14)N(13) 111.2(4), N(1)BN(10) 109.9(4), H(1A)BH(1B) 112(3), H(1A)BN(1)C(9) -11(2), H(1A)BN(10)C(11) 65(2), H(1B)BN(1)C(2) 48(5), H(1B)BN(10)C(14) 8(2)

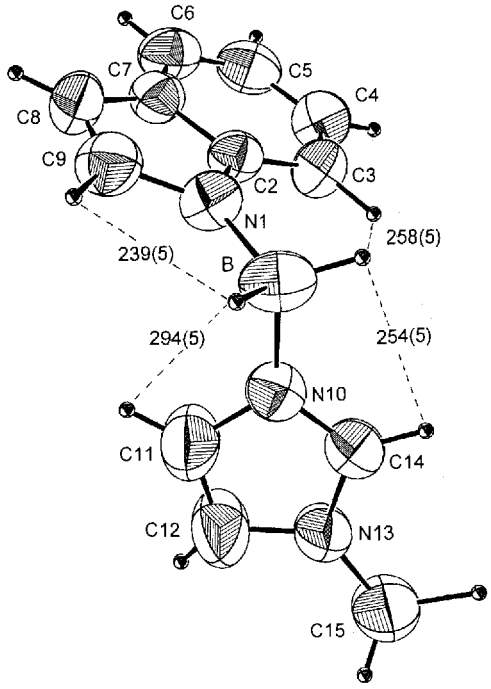

Figure 4. Molecular structure of carbazolylborane-pyridine adduct **3c**. Bond lengths [pm] and bond angles [°]: N(1)-B(1) 160.7(6), N(2)-B(1) 152.1(7), C(11)-C(12) 143.2(6), B(1)-H(17) 115(4), B(1)-H(18) 111(7), C(1)N(1)C(5) 117.3(4), C(1)N(1)B(1) 122.2(4), C(5)N(1)B(1) 120.5(4), C(6)N(2)C(17) 106.2(4), C(6)N(2)B(1) 128.1(4), C(17)N(2)B(1) 125.5(4), C(6)C(11)C(12) 106.3(4), C(11)C(12)C(17) 119.4(5), N(1)B(1)N(2) 107.8(4), H(17)B(1)H(18) 115(4), H(17)B(1)N(2)C(17) -44(3), H(17)B(1)N(1)C(1) -6(3), H(18)B(1)N(2)C(6) 12(3), H(18)B(1)N(1)C(5) -63(3)

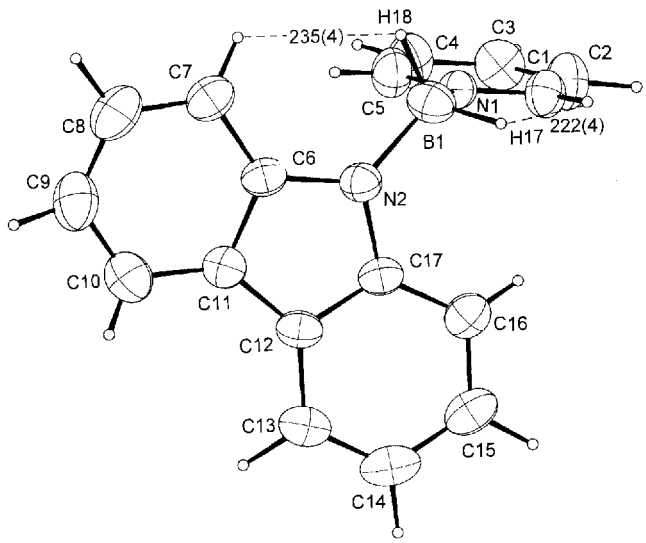

lengths of the carbon atoms β to the pyrrolic-type nitrogen are shorter and the C–N–C angles are smaller than in pyr-

Figure 5. Molecular structure of carbazolylborane-N-methyl-imidazole adduct **3d**. Bond lengths [pm] and bond angles [°]: N(1)-C(1) 132.4(5), N(1)-C(2) 135.4(5), N(2)-C(1) 131.2(5), N(2)-C(3) 135.9(5), N(2)-B(1) 158.3(6), N(3)-B(1) 153.0(6), C(2)-C(3) 132.9(6), C(10)-C(11) 143.7(5), B(1)-H(17) 112(4), B(1)-H(16) 118(7), C(1)N(1)C(2) 107.3(4), C(1)N(2)C(3) 105.8(4), C(1)N(2)B(1) 127.6(4), C(3)N(2)B(1) 126.6(4), C(5)N(3)C(16) 106.6(3), C(5)N(3)B(1) 127.7(3), C(16)N(3)B(1) 124.9(3), N(1)-C(1)N(2) 110.8(4), N(1)C(2)C(3) 106.7(4), N(2)C(3)C(2) 109.4(4), C(5)C(10)C(11) 106.1(3), C(10)C(11)C(16) 106.6(3), N(2)B(1)N(3) 107.4(3), H(17)B(1)H(16) 112(3), H(16)B(1)N(3)C(16) 45(3), H(16)B(1)N(2)C(1) -2(3), H(17)B(1)N(3)C(5) -23(3), H(17)B(1)N(2)C(3) 58(3)

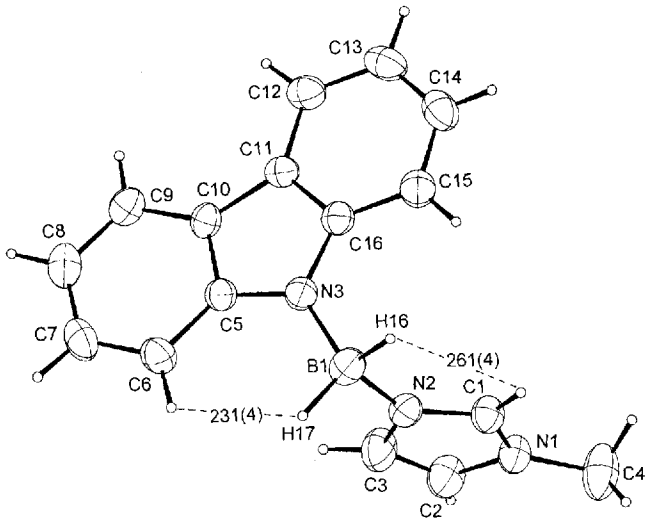

Table 1. Interatomic distances [pm] and angles [°] of azolylborane adducts **1c**, **1e**, **2d**, **3c**, and **3d**

compounds	N-B	N→B	N→B-N	H-B-H	Cβ-Cβ[b]	C-N-C[a]
pyrrolylborane-pyridine **1c**	152.8(6)	161.9(5)	108.7(3)	116(3)	138.5(7)	106.6(4)
pyrrolylborane-imidazole **1e**	151.4(4)	157.5(4)	109.8(2)	113(3)	136.4(4)	105.7(2)
indolylborane-N-methyl-imidazole **2d**	150.3(6)	158.0(7)	109.9(4)	112(3)	141.9(7)	104.6(3)
carbazolylborane-pyridine **3c**	152.1(7)	160.7(6)	107.8(4)	115(4)	143.2(6)	106.2(4)
carbazolylborane-N-methyl-imidazole **3d**	153.0(6)	158.3(6)	107.4(3)	112(3)	143.7(5)	106.6(3)

[a] Azolyl ring. – [b] β Carbon atoms to the pyrrolic-type nitrogen.

role [141.0(18) pm, 109.4(4)°][7], indole [(143.6(18) pm, 108.9(15)°][7], or carbazole [147.7(1), 108.3(5)°][8] free heterocycles. The structure of the imidazole ring[9] changes significantly upon coordination, the C4′–C5′ bond length becomes shorter which suggests the localization of the C4′–C5′ double bond (Table 2). The N1′–C2′ and C2′–N3′ bond distances become similar indicating a tricentric delocalized allylic-type bond N1′–C2′–N3′ in the coordinated compounds (atom numbering according to Scheme 1).

In compounds **1c** and **1e** the smaller size of the pyrrole ring allows a conformation which makes the hydric hydrogen to get close to their neighbouring protic hydrogen in both heterocycles. The B–H bonds are almost in the plane of both heterocycles, the dihedral angles between the B–H bonds and the ring planes are smaller than expected. For the pyrrolylborane–imidazole complex **1e** (Figure 2) the bond lengths are: $H1^{\delta+}\ldots{}^{\delta-}H9$ = 258.4(3), $H7^{\delta+}\ldots{}^{\delta-}H9$ =

Table 2. Interatomic distances [pm] and angles [°] related to the imidazole ring of azolylborane adducts **1e**, **2d**, and **3d**

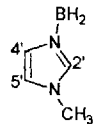

compounds	N1′-C2′	C2′-N3′	N3′-C4′	C4′-C5′	N1′-C5′	C2′N3′C4′
imidazole e[a]	134.9(5)	132.6(5)	137.8(5)	135.8(5)	136.9(5)	105.4(3)
pyrrolylborane-imidazole **1e**	133.6(3)	131.6(3)	134.6(3)	130.7(3)	133.1(3)	105.7(2)
indolylborane-N-methyl-imidazole **2d**	132.0(6)	130.1(5)	135.7(6)	132.0(8)	135.4(7)	106.2(4)
carbazolylborane-N-methyl-imidazole **3d**	132.4(5)	131.2(5)	135.9(5)	132.9(6)	135.4(5)	105.8(4)

[a] N–H instead of N–CH_3, ref.[9].

251.8(3), $H3^{\delta+}\ldots{}^{\delta-}H10$ = 262.7(3), and $H4^{\delta+}\ldots{}^{\delta-}H10$ = 262.5(3) pm. The dihedral angle values are: H9–B1–N3–C7 = –23.6(3), H9–B1–N2–C1 = 31.3(3), H10–B1–N3–C4 = 34.5, and H10–B1–N2–C3 = –29.2(3)°. The exocyclic angles H7–C7–N3 [117.2(4)°] and H4–C4–N3 [116.5(4)°] of pyrrole are closer than in free pyrrole (121.5°)[7]. The exocyclic angles near the hydrides H1–C1–N2 [122.1(4)°] and H3–C3–N2 [119.3(4)°] in imidazole are also smaller than in free imidazole (124.5 and 122.2°, respectively)[9]. The proximity of hydric hydrogen and acidic hydrogen denotes a hydric-protic interaction. An important result is that the conformation of the pyrrolylborane–pyridine adduct **1c** (Figure 1) is not in agreement with the ab initio-calculated preferred conformer[10], in which the two rings are in orthogonal position.

In the indolylborane **2d** (Figure 3) and carbazolylborane **3d** (Figure 5) *N*-methylimidazole complexes the increased steric demand of the azolyl ring makes them to adopt a conformation with the shortest distance between one of the hydric atoms and the more acidic hydrogen (H14 in **2d** and H16 in **3d**).

The observed preferred conformations in the solid state afford evidence of hydrogen bonding between protic hydrogens and hydric hydrogens. The hydrogen atoms bound to carbon atoms α to the nitrogen have an acidic character which increases upon nitrogen coordination[11,12]. The Mulliken-calculated charges for hydrogen, carbon, and boron atoms in free imidazole, *N*-coordinated imidazole, and imidazolium salts are given in Table 3. The interaction between hydric vs protic atoms could be described as a hydrogen bonding[13–20], shorter distances than 265 pm could be considered as contact distances[21–24].

In adduct **1e** (Figure 2) there are four contact lengths for protic-hydric atoms $C{-}H^{\delta+}\ldots{}^{\delta-}H{-}B$ which depict four five-membered rings and two tricentric interactions: $H1^{\delta+}\ldots{}^{\delta-}H9\ldots{}^{\delta+}H7$ and $H3^{\delta+}\ldots{}^{\delta-}H10\ldots{}^{\delta+}H4$. The pyrrolylborane–pyridine adduct **1c** (Figure 1) shows a similar behaviour. In adducts derived from indole **2d** (Figure 3) and carbazole **3c** and **3d** (Figures 4 and 5) the larger size of the azolyl ring does not allow tricentric interactions, but the dicentric ($C{-}H^{\delta+}\ldots{}^{\delta-}H{-}B$) are present. In **2d** (Figure 3)

there are two contact lengths: $H9^{\delta+}...^{\delta-}H1A$ = 239(5) and $H14^{\delta+}...^{\delta-}H1B$ = 254(5) pm in five-membered rings and one $H3^{\delta+}...^{\delta-}H1B$ = 258(5) pm in a six-membered ring. The distance $H11^{\delta+}...^{\delta-}H1A$ = 294(5) pm, which has a wide dihedral angle, is excluded as a contact length [H1A−B−N10−C11 = 65(2)°]. In **3c** and **3d** the same behaviour is observed (Figures 4 and 5, respectively).

Table 3. Mulliken total atomic charges [*e*] of *N*-methylimidazole N→BH_3, N→BF_3, and N^+−H adducts ab initio-calculated at 6-31G** level (numbering according to Scheme 1)

atom	N→BH_3 adduct	N→BF_3 adduct	imidazolium cation
2'-H bonded to C-2'	0.210	0.227	0.271
C-2'	0.429	0.443	0.472
4'-H bonded to C-4'	0.198	0.215	0.260
C-4'	0.070	0.080	0.080
H bonded to B	-0.18		
F bonded to B		-0.43	

A similar interaction was found between imidazole protons and fluorine atoms of the BF_3 adduct of imidazole (Figure 6). The fluorine atom F9 is almost coplanar with the imidazole ring (F9B6N3C2 = 11.7°), the exocyclic angle H2C2N3 = 119(3)° is closed toward the fluorine. The intramolecular distance $F9^{\delta+}...^{\delta-}H2$ [249(4) pm] is shorter than the sum of the van der Waals radii of hydrogen and fluorine (r_{VDW} H = 120 pm; r_{VDW} F = 150−160[25], 135[26]). In addition, the intermolecular distance $F9^{\delta-}...^{\delta+}H2'$ of 249(4) pm is closer to a short contact, and both atoms are almost colinear [B6−$F9^{\delta-}...^{\delta+}$H2' angle 170(4)°]. The net atomic charges calculated ab initio for the *N*-methylimidazole N→BF_3 adduct are shown in Table 3. It was observed by X-ray diffraction analysis that the H2' of the imidazole ring forms hydrogen bonds with some anions in imidazolium salts, and that the arrangement C2−H2...X is almost linear for X = Cl, I, C(carbene)[27]. Some F...H intermolecular interactions in BF_3 complexes were also found[28−32].

Figure 6. Molecular structure of BF_3-imidazole adduct. Bond lengths [pm] and bond angles [°]: N(1)C(2) 131.0(6), N(1)-C(5) 136.7(8), N(3)-C(2) 130.6(7), N(3)-C(4) 137.7(6), C(4)-C(5) 133.4(7), N(3)B(6) 154.4(7), F(7)-B(6) 137.9(9), F(8)-B(6) 137.8(8), F(9)-B(6) 135.4(9), C(2)N(1)C(5) 109.4(5), C(2)N(3)C(4) 106.7(4), N(1)C(2)N(3) 109.8(5), N(3)C(4)C(5) 108.9(5), N(1)C(5)C(4) 105.2(5), C(2)N(3)B(6) 126.1(5), C(4)N(3)B(6) 127.3(5), F(7)B(6)N(3) 108.8(5), F(8)B(6)N(3) 108.1(5), F(9)B(6)N(3) 110.0(5), B(6)F(9)H(2') 170(3)

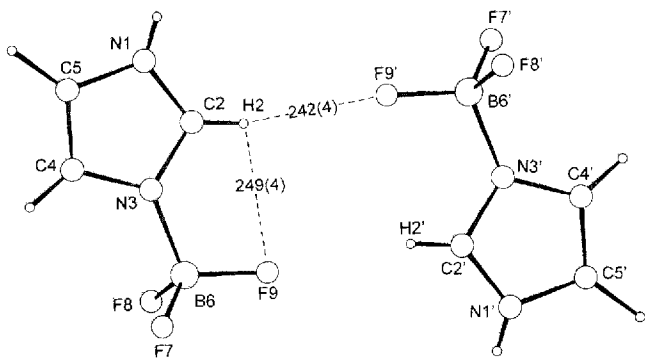

NMR Studies in Solution

The weak THF complexes (**1b−3b**) were not isolated, they were directly studied in the THF solution, and in order to have similar conditions with the other complexes they were dissolved in [D_8]THF.

^{11}B NMR: The weak THF complexes of azolylboranes **A** may exist in equilibrium with the free azolylboranes **B**, which in turn have a resonance structure **C** (Scheme 2). The contribution of the latter depends on: (a) The coplanarity of the $-BH_2-$ group and the aromatic ring, (b) the azolyl electronic withdrawal effect on the π electronic density of the N−B bond, and (c) the steric demand.

Scheme 2. Equilibrium in solution of the azolylborane−THF complexes **1b** and **2b**

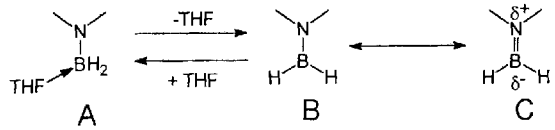

The aromatic character of the heterocycles decreases in the order carbazole (resonance energy 1379.4 kJ mol^{-1})[33], indole (760.8), and pyrrole (376.2). In consequence the acidity of the boron atom decreases in the order pyrrolylborane, indolylborane, and carbazolylborane. From these data it can be concluded that in the less aromatic heterocycle, the pyrrolylborane−THF complex **1b**, the N−B-retrocoordinated bond (structure **C**) could be favoured over those of **2b** and **3b**. The ^{11}B-chemical shifts of pyrrolylborane−THF **1b** (δ = 4.2), indolylborane−THF **2b** (δ = 2.6), and carbazolylborane−THF **3b** (δ = 0.1) is in agreement with the steric demand of the azolyl ring and the electronic effect.

The Lewis acid character of the boron atom in these compounds has a direct relationship with the acidic character of N−H in the free heterocycles **1−3** (NH δ^1H: pyrrole 9.50, indole 10.02, and carbazole 10.70).

THF exchange by a stronger coordinating base as pyridine or imidazole shifts the δ^{11}B value to lower frequencies in agreement with the donor capacity of the Lewis base (Table 4). Therefore, the difference Δδ between the azolyl−THF complex and the pyridine or imidazole complexes is a measure of the nitrogen heterocyclic basicity. Thus, it appears that imidazole is a stronger donor than pyridine.

Table 4. ^{11}B-chemical shifts and ^1J(B,H) [Hz] values of azolylborane adducts **1b−3d** in [D_8]THF

	THF (b)		pyridine (c)			N-methyl-imidazole (d)		
azole	δ ^{11}B	^{1}J(B,H)	δ ^{11}B	Δδ ^{11}B[b]	^{1}J(B,H)	δ ^{11}B	Δδ ^{11}B[b]	^{1}J(B,H)
pyrrole (**1**)	4.3	[a]	-3.2	7.5	[a]	-7.8	12.1	102
indole (**2**)	2.6	[a]	-4.6	7.2	96	-9.5	12.1	[a]
carbazole (**3**)	0.1	[a]	-7.0	7.1	92	-11.4	11.5	97

[a] Broad signal. − [b] Δδ ^{11}B = [δ ^{11}B of THF adduct (**1b−3b**) − δ ^{11}B of heterocycle adduct (**1c−3c** and **1d−3d**)].

^{13}C NMR: The ^{13}C- and ^{1}H-NMR spectra of pyrrole[34], indole[34a,35], and carbazole[34a,36] are known. The ^{13}C- and ^{1}H-NMR data assignments of pyrrolylboranes **1a−e** are trivial. The close proximity of δ ^{13}C of C-4 and of C-6 in

the indolylboranes **2b**, **c** and δ^{13} of C-3(6) and of C-4(5) in the carbazolylboranes derivatives **3b–d** made necessary to carry out other experiments to unequivocally assign the ^{13}C- and ^{1}H-NMR chemical shifts. This was achieved by NMR heteronuclear correlation ^{1}H-^{13}C and selective homonuclear irradiation spectra (^{1}H NMR).

It is known that NMR may give information about the electronic changes produced by coordination of the nitrogen in pyridine[37] and imidazole[38] rings. In the pyridine ring $\delta^{13}C$ of C-4′ is shifted to higher frequencies by electronic effects (**1c–3c**, Table 5). It was established that this $\Delta\delta^{13}C$ of C-4′ allows to evaluate the bonding strength of the N→B bond[37]. In imidazole the same electronic effect is observed at C-4′[38] (**1d–3d**, Table 5). The same trends are followed by the ^{1}J(C,H) values[39] of all carbon atoms which became larger due to the electroattractive effect of borane. The observed effects indicate the acid strength order: $BH_3 < N-BH_2 < BF_3$. We could not discern a difference between the three studied azolylboranes.

Table 5. ^{13}C-NMR data of pyridine and *N*-methylimidazole rings of azolylborane complexes **1c–3d** in [D$_8$]THF (^{1}J(C–H) [Hz] in parentheses)

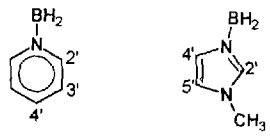

	pyridine (**c**) $\delta^{13}C$ [^{1}J(C,H)]			N-methyl-imidazole (**d**) $\delta^{13}C$ [^{1}J(C,H)]			
azolyl	C-2′	C-3′	C-4′	C-2′	C-4′	C-5′	N-CH$_3$
none	149.8[a,b] (177.6)	123.7[a,b] (163.0)	135.9[a,b] (162.4)	138.6 (206)	129.7 (189)	120.6 (189)	33.1
pyrrolylborane (**1**)	145.9 (185.7)	126.9 (170.1)	141.7 (167.4)	137.5 (218)	125.5 (195)	122.5 (196)	34.6
indolylborane (**2**)	146.2 (185.2)	126.8 (170.5)	141.7 (166.7)	137.5 (215)	125.6 (196)	122.5 (195)	34.5
carbazolylborane (**3**)	146.0 (182.2)	127.1 (170.3)	141.9 (166.3)	137.5 (216)	125.2 (196)	122.6 (197)	34.6
BH_3	147.3[a]	125.7[a]	139.5[a]	136.9[c] (214)	127.1[c] (196)	121.5[c] (196)	34.9[c]
BF_3	143.2[a]	126.2[a]	143.4[a]	135.3[c] (215)	123.5[c] (199)	121.6[c] (197)	35.3[c]

[a] Ref.[37]. – [b] Ref.[39]. – [c] Ref.[38].

In the azolyl–THF complexes $\delta^{13}C$ of C-2, C-7a, C-3, and C-4a resonances in the indolylborane **2b** and C-4a(5a) and C-8a(9a) in the carbazolylborane **3b** are shifted to higher frequencies upon borane coordination. A similar behaviour is found in silicon and tin derivatives of **1a–3a**[40] which indicates the electrodeficient nature of the boron atom and the weak electron donating ability of THF.

Carbazole and indole rings could be considered as substituted anilines, $\delta^{13}C$-5 of indole and $\delta^{13}C$-3(6) of carbazole (both *para* to N–BH$_2$–) are sensitive to resonance and inductive effects (Table 6)[36c]. The shift to lower frequencies of these carbon atoms signals suggests that the N→BH$_2$ bonding increases the electronic density in the azolyl ring. This was confirmed by the ^{1}J(C,H) values of C2–H and C3–H of pyrrole compounds **1b–1d** which diminish upon boron bonding in the order THF > pyridine > *N*-methylimidazole. The effect is less evident in carbazole and indole rings because the charge is redistributed through the rings. In contrast with the azolyl–THF complexes, the azolyl–pyridine and azolyl–*N*-methylimidazole adducts show more participation in the π system of the lone pair of pyrrole type nitrogen (N–B), allowing a dipole with a partial negative charge in the azolyl and a partial positive charge in the coordinating heterocycle (Scheme 3).

Scheme 3. Charge density distribution of pyrrolylborane–*N*-methylimidazole adduct **1d**

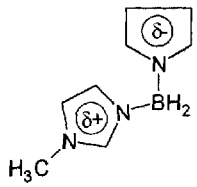

Table 6. ^{13}C-NMR data of pyrrole, indole, and carbazole rings of azolylborane adducts **1a–3d** in [D$_8$]THF (^{1}J(C,H) [Hz] in parentheses)

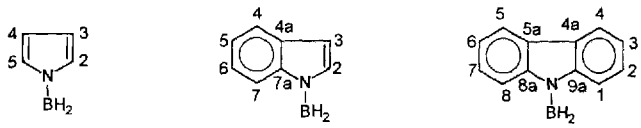

pyrrole or indole ring	C-2 ^{1}J(C2,H)	C-3 ^{1}J(C3,H)	C-4 ^{1}J(C4,H)	C-5 ^{1}J(C5,H)	C-6 ^{1}J(C6,H)	C-7 ^{1}J(C7,H)	C-3a	C-7a
pyrrole **1a**	118.0 (182.5)	108.0 (168.5)						
pyrrolylborane-THF **1b**	124.0 (180.6)	109.8 (166.9)						
pyrrolylborane-pyridine **1c**	125.8 (177.1)	109.2 (166.0)						
pyrrolylborane-N-methyl-imidazole **1d**	125.4 (n.m)[a]	108.0 (164.3)						
indole **2a**	125.0 (181.3)	102.2 (171.7)	119.1 (157.3)	120.9 (156.6)	121.8 (159.0)	111.7 (160.1)	129.1	137.3
indolylborane-THF **2b**	134.5 (178.1)	102.4 (169.7)	120.3 (156.4)	119.1 (156.4)	120.8 (156.4)	112.7 (157.9)	131.6	141.5
indolylborane-pyridine **2c**	134.5 (177.5)	101.6 (169.3)	120.4 (162.1)	118.7 (156.2)	120.6 (156.4)	112.7 (157.5)	131.8	141.3
indolylborane-N-methyl-imidazole **2d**	134.6 (182)	100.6 (169)	120.4 (155)	118.1 (156)	119.9 (155)	112.9 (157)	131.6	141.4

carbazole ring	C-4(5)	C-3(6)	C-2(7)	C-1(8)	C-4a(5a)	C-8a(9a)
carbazole **3a**	120.7 (158.0)	119.4 (159.0)	126.1 (158.6)	111.3 (160.0)	122.7	140.9
carbazolylborane -THF **3b**	120.0 (157.2)	119.0 (159.2)	126.9 (156.5)	112.5 (158.3)	125.5	146.0
carbazolylborane -pyridine **3c**	120.1 (156.4)	118.4 (158.9)	125.4 (156.4)	112.4 (157.9)	125.5	146.1
carbazolylborane -N-methyl-imidazole **3d**	119.9 (156.3)	117.7 (158.9)	125.0 (157.0)	112.6 (158.9)	125.7	146.4

[a] n.m.: not measured.

^{1}H NMR: The spatial proximity of the hydric and protic hydrogens in solution was confirmed by NOE differential experiments[41] for pyridine and *N*-methylimidazole complexes of pyrrole (**1c**, **1d**), indole (**2c**, **2d**), and carbazole (**3c**, **3d**). The hydric hydrogens were irradiated and the ^{1}H-NMR spectra observed. In the indolylborane–*N*-methylimidazole adduct **2d** a NOE between the hydric hydrogens and the *N*-methylimidazole H2′, H4′ protic hydrogens and

the indole H2, H7 protic hydrogens is observed. A similar result was found for compounds **1c**, **1d**, and **2c** which confirms the preferred conformation of the azolylboranes.

For the carbazolylborane adducts **3c** and **3d**, there is only a NOE at 30°C between the hydride and the hydrogen atom H1(8) of the carbazole ring (Figure 7b). The N–B bond rotation is restricted by the large size of the carbazole whereas the coordinating heterocycle has a free rotation. This behaviour allows a longer contact time of H1(8) with the hydric hydrogens. The experiment at lower temperature (−90°C) shows the expected NOEs between the hydric hydrogens and the H2′ protic hydrogens of pyridine (**3c**) (Figure 7d), and a similar effect was found for hydric atoms and H2′, H4′ of *N*-methylimidazole (**3d**). This means that on decreasing the molecular movement the synchrony of both rings is retained increasing the population of the conformers with hydric-protic interactions.

Figure 7. [a] ^{1}H-NMR spectrum of **3c** at 30°C; [b] NOE differential spectrum of **3c** at 30°C; [c] ^{1}H spectrum of **3c** at −80°C; [d] NOE differential spectrum of **3c** at −80°C. * These signals correspond to pyridine–BH_3 adduct which became important due to the low solubility of **3c** at low temperature

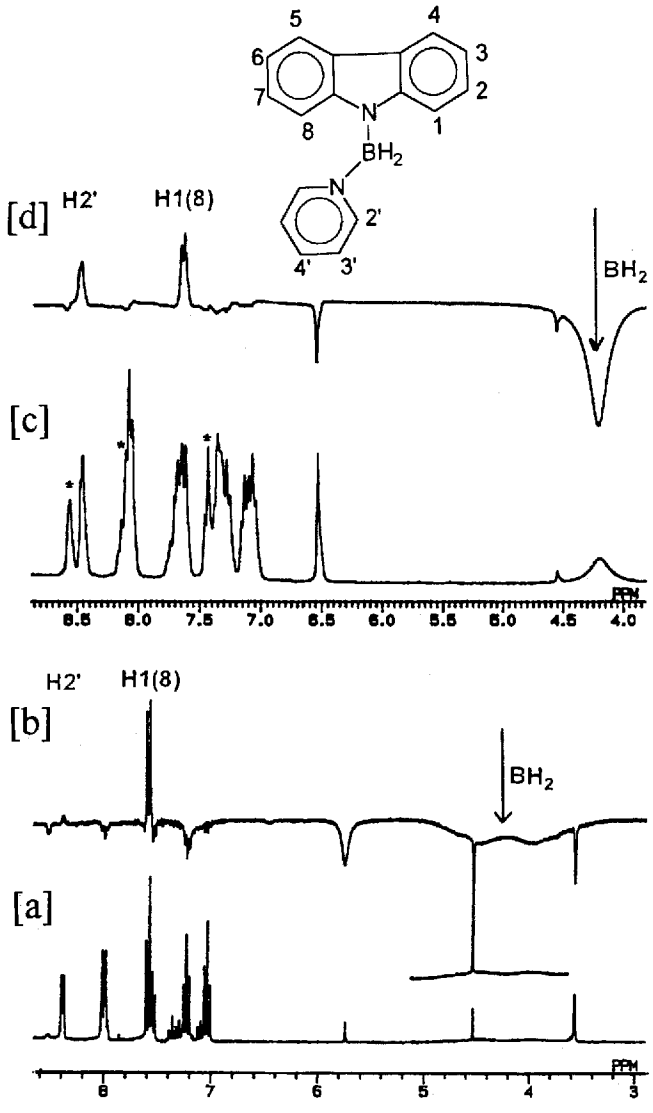

In order to confirm that the NOE was a consequence of a defined geometry[41b–d] we have performed a differential NOE irradiating H2′ of **1c** at −80°C. This irradiation generated a NOE on H3′ and H2(5) indicating that they have a preferred conformer similar to that observed in the structure obtained by X-ray diffraction. The (B)–H–H2(5) estimated angle based on NOE experiments was of 77(4)° (Figure 8). Similar results allow us to infer that pyrrole and pyridine rings in **1c** have a synchronic movement between the preferred conformations of the lowest energy **A′** and **A′** which are in equilibrium via conformer **A** (Scheme 4).

Scheme 4. Pyrrole and pyridine ring synchronic movement in pyrrolylborane–pyridine adduct **1c**. Broad lines in the pyridine ring represent out of plane bonds and broad lines of the pyrrole ring represent N1–C2(5) bonds

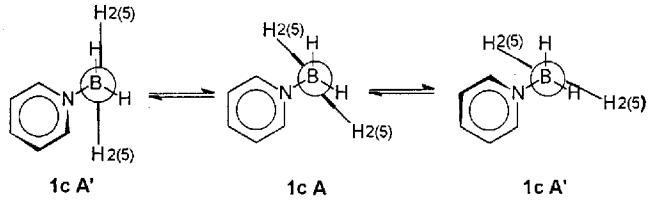

Figure 8. [a] Non-irradiated ^{1}H-NMR spectrum of **1c** at −80°C; [b] NOE differential spectrum of **1c** irradiated at the $-BH_2-$ frequency; [c] NOE differential spectrum of **1c** irradiated at the H2′ frequency

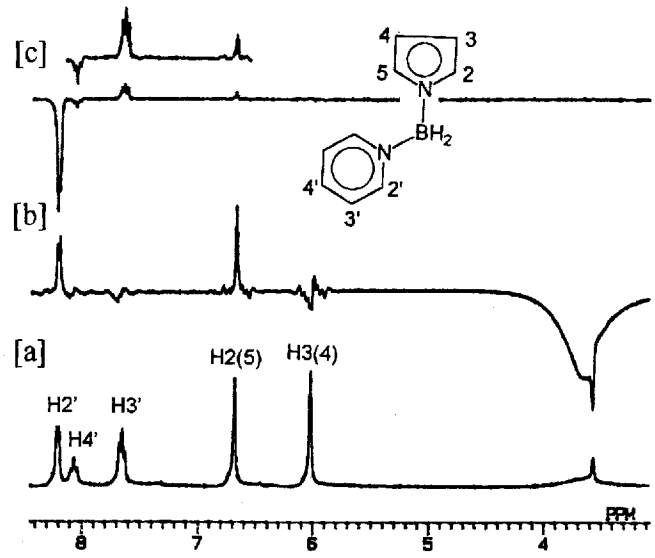

Conclusions

The X-ray diffraction structures of **1d**, **1e**, **2d**, **3c**, and **3d** showed preferred conformations in the solid state which give evidence of hydrogen bonding between protic hydrogens and hydric hydrogens.

The ^{13}C-NMR spectra afforded evidence of a betaine-type structure with a partial positive charge delocalized through the coordinating heterocycle and with a partial negative charge delocalized in the azolyl ring.

The differential NOE experiments allowed us to establish the spatial proximity of the hydrides with the protons in

the heterocycles and a synchronized movement in adducts **1c–2d** at room temperature which favors the conformations which get hydrides and protons closer. The synchrony of the rotational isomers for adducts **3c** and **3d** at room temperature is lost owing to the carbazole size, but it is recovered at low temperature (−80 °C).

The positive charge of H2′ protons in the adducts N→BH_3, N→BF_3, and N^+–H of *N*-methylimidazole, the negative charge of hydrides, the proximity of these hydrogen atoms, and the angle deformations allow us to propose the existence of hydrogen bonding both in the solid state and in solution.

We thank *Conacyt-Mexico* for the scholarship of I.I.P.-M. and Professor *A. Paz-Sandoval* for critical reading.

Experimental

All compounds were handled under N_2 by using carefully dried glassware and dry solvents. Starting materials such as pyrrole, indole, carbazole, *N*-methylimidazole, imidazole, and pyridine were commercial products. A BH_3 · THF solution and the imidazole–BF_3 adduct[38] were prepared according to reported methods[42]. – Melting points (uncorrected): Gallenkamp apparatus. – IR (KBr): Perkin Elmer 16F PC. – $^1H/^{13}C$ NMR: Jeol GXS 270 (270.67/67.94 MHz), TMS as external standard. Experimental conditions for NOE differential spectra were optimized for each compound at 30 and −80 °C: pulse width 90°, times 32–64, acquisition time 2.34–3.42 s, time delay 5–25 s, attenuator 200–350 over an attenuator scale of 500. – ^{11}B NMR: Jeol GXS 270 (86.84 MHz), Et_2O · BF_3 as external standard ($\Xi^{11}B$ = 32.083971 MHz). – ^{15}N NMR: Jeol GSX 270 (27.25 MHz), neat $MeNO_2$ as external standard ($\Xi^{15}N$ = 10136757 MHz). The refocused INEPT pulse sequence was used to detect ^{15}N signals by using $^2J(^{15}N,H2')$ between 8 and 10 Hz. – Elemental analyses: Oneida Research Services, Whitesboro, N.Y.

1. *Pyrrolylborane–THF Adduct* **1b**: 2.13 g (0.0317 mol) of freshly dried and distilled pyrrole was added dropwise to 14.4 ml of BH_3 · THF (2.20 M, 0.0317 mol) with vigorous stirring. The mixture was maintained in an ice-water bath. The reaction was followed by H_2 evolution using a gasimeter. After 4 h **1b** was obtained in 80% yield (0.0254 mol)[1a]. – ^1H NMR ([D$_8$]THF): δ = 6.84 [m, *J* = 1.7 and 2.2 Hz, 2H, 2(5)-H], 6.08 [m, *J* = 6.0, 2.2, and 1.7 Hz, 2H, 3(4)-H].

2. *Pyrrolylborane–Pyridine Adduct* **1c**: 2.01 g (0.0254 mol) of freshly dried and distilled pyridine was added to **1b** with agitation in an ice-water bath for 2 h. The mixture was stored at −20 °C during 15 d. After that time crystals suitable for X-ray analysis were isolated. Repeated crystallization from THF (−20 °C) yielded 3.20 g (64%) of **1c** as a white crystalline solid, m.p. 91–92 °C. – ^1H NMR ([D$_8$]THF): δ = 8.2 (dd, *J* = 5.3 and 1.5 Hz, 2H, 2′-H), 8.04 (dd, *J* = 7.7 and 1.5 Hz, 2H, 4′-H), 7.61 (dd, *J* = 7.7 and 5.3 Hz, 2H, 3′-H), 6.65 [m, *J* = 1.0 and 2.4 Hz, 2H, 2(5)-H], 6.07 [m, *J* = 1.0, 2.4 and 5.9 Hz, 2H, 3(4)-H]. – $C_9H_{11}BN_2$ (158.0): calcd. C 68.40, H 6.97, N 17.74; found C 69.00, H 6.96, N 17.95. – IR (KBr): $\tilde{\nu}$ = 2346 and 2288 cm^{-1} (B–H), 1622 (C=N), 1180 and 1098 (B–N).

3. *Pyrrolylborane–N-Methylimidazole Adduct* **1d**: A similar reaction as for **1c** was performed with 2.09 g (0.0254 mol) of *N*-methylimidazole and **1b** (0.0254 mol); yield 3.2 g of **1d** (63%) as a white crystalline solid. – ^1H NMR ([D$_8$]THF): δ = 7.71 (dd, *J* = 1.6 and 1.6 Hz, 1H, 2′-H), 6.95 (dd, *J* = 1.6 and 1.6 Hz, 1H, 5′-H), 6.90 (dd, *J* = 1.6 and 1.6 Hz, 1H, 4′-H), 6.59 [m, *J* = 2.4 and 1.0 Hz, 2H, 2(5)-H], 5.81 [m, *J* = 5.9, 2.4 and 1.0 Hz, 2H, 3(4)-H], 3.58 (s, 3H, NCH_3). – $C_8H_{12}BN_3$ (161.0): calcd. C 59.71, H 7.46, N 26.12; found C 59.50, H 7.32, N 26.30. – IR (KBr): $\tilde{\nu}$ = 2400 (B–H) cm^{-1}, 1605 (C=N), 1535 (C=C), 1172, 1135 (B–N). – ^{15}N NMR ([D$_8$]THF): δ = −172.0 (s, N→BH_2), −199.6 (b, NBH_2), −213.3 (s, NCH_3).

4. *Pyrrolylborane–Imidazole Adduct* **1e**: A similar reaction as for **1c** was performed with 1.73 g (0.0254 mol) of imidazole and **1b** (0.0254 mol); yield 2.80 g of **1e** (60%) as a white crystalline solid, m.p. 126–127 °C (dec.). – ^1H NMR ([D$_8$]THF): δ = 7.76 (s, 1H, 2′-H), 12.0 (br., 1H, NH), 7.05 (t, 1H, ^3J = 1.6, ^4J = 1.4 Hz, 5′-H), 6.95 (t, 1H, ^3J = 1.6, ^4J = 1.4 Hz, 4′-H), 6.60 (t, 2H, ^3J = 2.1, ^4J = 1.8 Hz, 2-H), 5.90 (t, 2H, ^3J = 2.1, ^4J = 1.8 Hz, 3-H), 3.4 (br. q, 3H, BH). – ^{13}C NMR ([D$_8$]THF): δ = 135.5 (C-2′), 125.5 (C-4′), 125.0 (C-2,5), 118.5 (C-5′), 107.9 (C-3,4). – ^{11}B NMR ([D$_8$]THF): δ = −7.8 (q, ^1J = 99 Hz). – $C_7H_{10}BN_3$ (147.0): calcd. C 57.20, H 6.86, N 28.59; found C 57.21, H 6.58, N 28.82. – IR (KBr): $\tilde{\nu}$ = 2378 cm^{-1} (B–H), 1684 (C=N), 1156 and 1080 (B–N).

5. *Indolylborane–THF Adduct* **2b**: A solution of 2.00 g (0.0171 mol) of freshly dried and distilled indole in 1 ml of dry THF was added dropwise to 7.80 ml of BH_3 · THF (2.2 M, 0.0171 mol) with vigorous stirring. The mixture was maintained in an ice-water bath. The reaction was followed by H_2 evolution by using a gasimeter, after 2 h **2b** was obtained (90%, 0.0154 mol). – ^1H NMR ([D^8]THF): δ = 7.53 (m, *J* = 7.8, 1.4, and 1.4 Hz, 1H, 7-H), 7.46 (dd, *J* = 8.1 and 1.4 Hz, 1H, 4-H), 7.14 (d, *J* = 3.0 Hz, 1H, 2-H), 7.00 (m, *J* = 7.8, 7.0, and 1.4 Hz, 1H, 6-H), 6.91 (m, *J* = 8.1, 7.0, and 1.4 Hz, 1H, 5-H), 6.36 (dd, *J* = 3.0 and 1.4 Hz, 1H, 3-H).

6. *Indolylborane–Pyridine Adduct* **2c**: 1.22 g of freshly dried and distilled pyridine was added to **2b** (0.0154). After 2 h 5 ml of THF was evaporated in vacuo, and the mixture was maintained at the ice-water bath temp. The solution was left at −20 °C during 15 d, after this time 1.40 g (40%) of **2c** was obtained by filtration as a pale yellow crystalline solid, m.p. 117 °C (dec.). Crystals suitable for X-ray analysis were obtained after repeated crystallization from THF at −20 °C. – ^1H NMR ([D$_8$]THF): δ = 8.25 (dd, *J* = 6.6 and 1.5 Hz, 2H, 2′-H), 7.85 (dd, *J* = 7.7 and 1.5 Hz, 2H, 4′-H), 7.44 (dd, *J* = 7.7 and 6.6 Hz, 2H, 3′-H), 7.44 (m, *J* = 6.5, 1.5, and 0.7 Hz, 1H, 4-H), 7.36 (m, *J* = 7.2, 1.0, and 1.5 Hz, 1H, 7-H), 7.23 (dd, *J* = 3.0 and 0.7 Hz, 1H, 2-H), 6.93 (m, *J* = 7.2, 6.9, and 1.5 Hz, 1H, 6-H), 6.88 (m, *J* = 6.9, 6.5, and 1.5 Hz, 1H, 5-H), 6.38 (dd, *J* = 3.0 and 1.0 Hz, 1H, 3-H). – $C_{13}H_{13}BN_2$ (208.1): calcd. C 75.04, H 6.30, N 13.46; found C 74.90, H 6.42, N 13.52.

7. *Indolylborane–N-Methylimidazole Adduct* **2d** was obtained (1.80 g, 50%) from **2b** (0.0154 mol) and 1.26 g (0.0154 mol) of *N*-methylimidazole as a white crystalline solid, m.p. 117–119 °C. – ^1H NMR ([D$_8$]THF): δ = 7.76 (dd, *J* = 1.8 and 1.6 Hz, 1H, 2′-H), 7.42 (dd, *J* = 7.9 and 1.2 Hz, 1H, 4-H), 7.39 (m, *J* = 7.6, 0.7, and 1.3 Hz, 1H, 7-H), 7.18 (d, *J* = 2.9 Hz, 1H, 2-H), 6.87 (m, *J* = 7.9, 7.0, and 1.3 Hz, 1H, 5-H), 6.94 (dd, *J* = 1.8 and 1.6 Hz, 1H, 4′-H), 6.94 (dd, *J* = 1.6 and 1.6 Hz, 1H, 5′-H), 6.88 (dd, *J* = 6.6 and 1.5 Hz, 2H, 2′-H), 6.80 (m, *J* = 7.6, 7.0, and 1.2 Hz, 1H, 6-H), 6.30 (dd, *J* = 2.9 and 0.9 Hz, 1H, 3-H), 3.46 (s, 3H, NCH_3). – $C_{12}H_{14}BN_3$ (211.1): calcd. C 68.29, H 6.69, N 19.91; found C 67.71, H 6.72, N 19.70. – IR (KBr): $\tilde{\nu}$ = 2388 cm^{-1} (B–H), 1604 (C=N), 1550 (C=C), 1224, 1196 (B–N).

8. *Carbazolylborane–THF Adduct* **3b**: A solution of carbazole (2.00 g, 0.0120 mol) in 1 ml of dry THF was added dropwise to 5.5 ml of BH_3 · THF (2.20 M, 0.0120 mol) with vigorous stirring. The mixture was maintained in an ice-water bath. The reaction was followed by H_2 evolution by using a gasimeter, after 1 h compound **2c** was obtained (97%, 0.0116 mol). – ^1H NMR ([D$_8$]THF): δ =

Table 7. Crystallographic data for pyrrolylborane–pyridine **1d**, pyrrolylborane–imidazole **1e**, indolylborane–*N*-methylimidazole **2d**, carbazolylborane–pyridine **3c**, carbazolylborane–*N*-methylimidazole **3d**, and imidazole–BF_3 adducts

	1c	**1e**	**2d**	**3c**	**3d**	**imidazole-BF_3**
formula	$C_9H_{11}BN_2$	$C_7H_{10}N_3B$	$C_{12}H_{14}BN_3$	$C_{17}H_{15}BN_2$	$C_{16}H_{16}BN_3$	$C_3H_4BF_3N_2$
molecular mass [g/mol]	158.01	146.99	211.08	258.13	261.13	135.88
crystal system	monoclinic	monoclinic	monoclinic	trigonal (hexagonal axes)	trigonal (hexagonal axes)	monoclinic
space group	P $2_1/n$	P $2_1/n$	P $2_1/n$	R $\bar{3}$	R $\bar{3}$	P $2_1/a$
a [pm]	754.0 (1)	944.9 (1)	891.0 (3)	2885.5(3)	2838.9(1)	516.5(1)
b [pm]	1494.3 (1)	1152.8 (1)	1285.8 (7)	2884.5(3)	2839.2(7)	1633.2(1)
c [pm]	850.4 (1)	776.1 (1)	1079.4 (4)	901.2(1)	901.7(2)	674.9(1)
α [°]	90	90	90	90	90	90
β [°]	106.51 (8)	97.60 (6)	105.30 (3)	90	90	107.06(6)
γ [°]	90	90	90	120.0	120.0	90
V [nm^3]	9.186 (2)	8.368 (1)	11.927 (5)	64.49(1)	62.944(3)	5.442(1)
Z	4	4	4	18	18	4
d_{calcd} [g cm^{-3}]	1.14	1.17	1.18	1.19	1.19	1.66
scan range [°]	1.0 + 1.500 tan θ	0.7 + 0.345 tan θ	0.5 + 0.580 tan θ	0.58 + 0.54 tan θ	0.49 + 0.58 tan θ	0.5 + 0.960 tan θ
θ range [°]	1.4 - 25	3 - 19	1.4 - 26	2.17 - 25	1 - 25	1 - 20
reflexions measured	1791	1418	2670	1497	2628	540
unique reflexions	1791	656	2582	1433	2450	540
reflexions used with $(F_o)^2 > 3\sigma(F_o)^2$	936	548	1084	909[a]	1220	500
R (int)		0.03		1.39	1.50	
absorption correction, DIFABS [min, max]	0.66, 1.00	0.91, 1.06	0.713, 0.939	0.88, 1.14	0.87, 1.16	0.92, 0.998
$R = \Sigma(\|Fo\|-\|Fc\|)/\Sigma\|Fo\|$	0.066	0.028	0.059	0.044	0.045	0.062
$Rw = [\Sigma w(\|Fo\|-\|Fc\|)^2/\Sigma wFo^2]^{1/2}$	0.083	0.024	0.055	0.037	0.044	0.057
no. of variables	154	100	201	227	230	98
min res density [10^{-6} e/pm^3]	0.00	-0.11	-0.95	-0.29	-0.20	-0.41
max res density [10^{-6} e/pm^3]	0.45	0.18	7.41	0.38	0.44	0.37

[a] $(F_o)^2 > 2\sigma(F_o)^2$.

7.97 [d, J = 7.8 Hz, 2H, 4(5)-H], 7.69 [d, J = 8.3 Hz, 2H, 1(8)-H], 7.26 [dd, J = 8.3 and 7.2 Hz, 2H, 2(7)-H], 7.07 [dd, J = 7.8 and 7.2 Hz, 2H, 3(6)-H].

9. *Carbazolylborane–Pyridine Adduct* **3c**: Freshly dried and distilled pyridine 0.92 g was added to **3b** (0.0116 mol) with stirring during 2 h in an ice-water bath. The solution was left at −20°C for 7 d, then 2.80 g of **3c** was obtained as a white crystalline solid, m.p. 148–150°C (dec.). – ^{1}H NMR ([D$_8$]THF): δ = 8.35 (d, J = 5.3 Hz, 2H, 2′-H), 8.00 [dd, J = 7.7 and 1.3 Hz, 2H, 4(5)-H], 7.91 (d, J = 7.9 Hz, 2H, 4′-H), 7.60 [dd, J = 8.2 and 1.3 Hz, 2H, 1(8)-H], 7.47 (dd, J = 7.9 and 5.3 Hz, 2H, 3′-H), 7.24 [m, J = 8.2, 7.1, and 1.0 Hz, 2H, 2(7)-H], 7.04 [m, J = 7.7, 7.1, and 1.3 Hz, 2H, 3(6)-H]. – $C_{17}H_{15}BN_2$ (258.1): calcd. C 79.10, H 5.86, N 10.85; found C 79.59, H 5.92, N 10.74. – IR (KBr): $\tilde{\nu}$ = 2410 and 2354 cm^{-1} (B–H), 1684 (C=N), 1618 (C=C), 1154 (B–N).

10. *Carbazolylborane–N-Methylimidazole Adduct* **3d**: As **3c**, 3.23 g (90%) of **3d** was obtained from **3b** (0.0116 mol) and 0.95 g of *N*-methylimidazole as a white crystalline solid, m.p. 198–200°C. – ^{1}H NMR ([D$_8$]THF): δ = 7.95 [dd, J = 7.7 and 1.1 Hz, 2H, 4(5)-H], 7.78 (dd, J = 1.6 and 1.3 Hz, 1H, 2′-H), 7.66 [dd, J = 8.2 and 1.3 Hz, 2H, 1(8)-H], 7.21 [m, J = 7.1, 1.3, and 1.1 Hz, 2H, 2(7)-H], 7.03 (dd, J = 1.6 and 1.3 Hz, 1H, 5′-H), 6.98 [m, J = 7.7, 7.1, and 1.3 Hz, 2H, 3(6)-H], 6.96 (dd, J = 1.6 and 1.3 Hz, 1H, 4′-H), 3.51 (s, 3H, NCH_3). – $C_{16}H_{16}BN_3$ (261.1): calcd. C 73.59, H 6.18, N 16.09; found C 73.96, H 6.19, N 16.12. – IR (KBr): $\tilde{\nu}$ = 2390 and 2356 cm^{-1} (B–H), 1684 (C=N), 1558 (C=C), 1146 and 1154 (B–N). – ^{15}N NMR ([D$_8$]THF): δ = −173.8 (s, N→BH_2), −196.5 (b, NBH_2), −212.3 (s, NCH_3).

11. *Imidazole–BF_3 Adduct:* ^{15}N NMR ([D$_6$]DMSO): −177 [sept, ^1J(N,B) = 25, ^2J(N,F) = 25 Hz], −206 [m, ^nJ(N,H) = 12, ^nJ(N,H) = 6 Hz, NH].

12. *Structure Determinations of* **1c**, **1e**, **2d**, **3c** *and* **3d**: Suitable crystals were obtained from saturated THF solutions after 2 or 3 weeks at −20°C. The crystal data and refinement parameters are listed in Table 7. Geometry and intensity data were collected on an Enraf-Nonius CAD4 diffractometer, with Mo-K_α (71.073 pm) radiation, equipped with graphite monochromator at 297 K, the scan mode used was ω/2Θ. The structures were solved by direct methods using the MOLEN (**1c**, **2d** and imidazole–BF_3 adduct) or CRYSTALS (**1e**, **3c**, **3d**) programs. In all cases hydrogen atoms were located and refined isotropically, except for **3c** and **3d**, for them only the hydride atoms were located. The non-hydrogen atoms were refined anisotropically.

[1] [1a] M. Añez, G. Uribe, L. Mendoza, R. Contreras, *Synthesis* **1981**, 214–216. – [1b] Camacho-Camacho, Ph. D. Thesis, CINVESTAV, México, **1985**. – [1c] M. Añez, M. S. Thesis, CINVESTAV, México, **1978**. – [1d] L. Martínez-Martínez, M. S. Thesis, CINVESTAV, México, **1979**.

[2] [2a] S. L. Ioffe, A. A. Lyashenko, O. P. Shitov, V. V. Negrebetskii, *Khim. Gaterotsikl. Soedin* **1971**, *8*, 1056–1057. – [2b] B. Gyori, J. Emry, P. Szarvas, *Acta Chim. Acad. Sci. Hung.* **1975**, *86*, 235–248. – [2c] S. Trofimenko, *Acc. Chem. Res.* **1971**, *4*, 17–22. – [2d] S. Trofimenko, *Chem. Rev.* **1972**, *72*, 497–509.

[3] [3a] N. Farfán, R. Contreras, *Nouv. J. Chim.* **1982**, *6*, 269–272. – [3b] N. Farfán, R. Contreras, *J. Chem. Soc., Perkin. Trans. 2*, **1988**, 1787–1791. – [3c] H. Singh, R. Sarin, K. Singh, R. Contreras, G. Uribe, *Tetrahedron* **1989**, *45*, 5193–5202. – [3d] A. Flores-Parra, G. Cadenas-Pliego, L. M. Martínez-Aguilera, M. L. García-Nares, R.Contreras, *Chem. Ber.* **1993**, *126*, 863–867.

[4] A. Haaland, *Angew. Chem.* **1989**, *101*, 1017; *Angew. Chem. Int. Ed. Engl.* **1989**, *28*, 992–1007.

[5] [5a] H. Nöth, B. Wrackmeyer, *Chem. Ber.* **1973**, *106*, 1145–1164. – [5b] H. Nöth, H. Prigge, *Chem. Ber.* **1986**, *119*, 338–348. – [5c] D. Männig, H. Nöth, H. Prigge, A.-R. Rotsch, S. Gopinathan, J. W. Wilson, *J. Organomet. Chem.* **1986**, *310*, 1–20. –

[5d] H. Nöth, H. Prigge, A.-R. Rotsch, *Chem. Ber.* **1986**, *119*, 1361–1373.
[6] B. Wrackmeyer, *Ann. Rep. NMR Spec.* **1988**, *20*, 61–203.
[7] P. J. Chadwick in *Comprehensive Heterocyclic Chemistry* (Eds.: A. R. Katritzki, C. W. Rees), Pergamon Press, Oxford, **1984**, vol. 4, chapter 3.04, p. 161–162.
[8] M. Kurahashi, M. Fukuyo, A. Shimada, A. Furusaki, I. Nitta, *Bull. Chem. Soc. Jpn.* **1969**, *42*, 2174–2179.
[9] S. Martínez-Carrera, *Acta. Crystallogr.* **1966**, *20*, 783–789.
[10] I. I. Padilla-Martínez, J. Ireta, M. Galván, R. Contreras, unpublished results. The preferred conformer was calculated at HF/6-31G** ab initio level with the Gaussian 92 program.
[11] [11a] A. J. Arduengo III, R. L. Harlow, M. Kline, *J. Am. Chem. Soc.* **1991**, *113*, 361–363. – [11b] A. J. Arduengo III, M. Kline, J. C. Calabrese, F. Davidson, *J. Am. Chem. Soc.* **1991**, *113*, 9704–9705. – [11c] A. J. Arduengo III; H. V. R. Dias, R. L. Harlow, M. Kline, *J. Am. Chem. Soc.* **1992**, *114*, 5530–5534. – [11d] A. J. Arduengo III, H. V. R. Dias, J. C. Calabrese, F. Davidson, *J. Am. Chem. Soc.* **1992**, *114*, 9724–9725.
[12] I. I. Padilla-Martínez, M. J. Rosalez-Hoz, R. Contreras, S. Kerschl, B. Wrackmeyer, *Chem. Ber.* **1994**, *127*, 343–346.
[13] The hydrogen bonding definition is wide, the classical one involves acidic hydrogen atoms bound covalently to electronegative atoms such as O and N[14]. Another kind of interactions were reported: O–H···C, N–H···C[15], C–H···O[16], M^-···H–N^+[17], and recently some novel[18] proton-hydride interactions Ir–$H^{\delta-}$...$^{\delta+}$H–N[19] and Ir–$H^{\delta-}$...$^{\delta+}$H–O[20]. The hydrogen bonding could also describe the proton-hydride C–$H^{\delta+}$...$^{\delta-}$H–B and proton-fluoride C–$H^{\delta+}$...$^{\delta-}$F–B interactions described here.
[14] M. C. Etter, *Acc. Chem. Res.* **1990**, *23*, 120–126, and references cited therein.
[15] M. A. Viswamitra, R. Radhakrishnan, J. Bandekar, G. R. Desiraju, *J. Am. Chem. Soc.* **1993**, *115*, 4868–4869.
[16] [16a] G. R. Desiraju, *Acc. Chem. Res.* **1991**, *24*, 290–296. – [16b] T. Steiner, W. Saenger, *J. Am. Chem. Soc.* **1993**, *115*, 4540–4547.
[17] I. C. M. Wehman-Ooyevaar, D. M. Grove, H. Kooijman, P. Sluis, A. L. Spek, G. Koten, *J. Am.Chem. Soc.* **1992**, *114*, 9916–9924.
[18] E. Peris, J. C. Lee, J. R. Rambo, O. Eisenstein, R. H. Crabtree, *J. Am. Chem. Soc.* **1995**, *117*, 3485–3491.
[19] [19a] S. Park, R. Ramachandran, A. J. Lough, R. H. Morris, *J. Chem. Soc., Chem. Commun.* **1994**, 2201–2202. – [37b] A. J. Lough, S. Park, R. Ramachandran, R. H. Morris, *J. Am. Chem. Soc.* **1994**, *116*, 8356–8357. – [37c] J. C. Lee, Jr., E. Peris, A. L. Rheingold, R. H. Crabtree, *J. Am. Chem. Soc.* **1994**, *116*, 11014–11019.
[20] [20a] J. C. Lee, Jr., A. L. Rheingold, B. Muller, P. S. Pregosin, R. H. Crabtree, *J. Chem. Soc., Chem. Commun.* **1994**, 1021–1022. – [20c] D. Milstein, J. C. Calabrese, I. D. Williams, *J. Am. Chem. Soc.* **1986**, *108*, 6387–6389. – [20c] R. C. Stevens, R. Bau, D. Milstein, O. Blum, T. H. Koetlze, *J. Chem. Soc., Dalton Trans.* **1990**, 1429–1431.
[21] The van der Waals radius (r_{VDW}) for the hydrogen atom in C–H bonds is usually accepted to be 120[22] pm, but there are calculated values of 145[23a] and 165[23b] pm. The atoms with anionic character usually have longer van der Waals radii than the corresponding neutral or cationic ones. In the metallic hydrides the H ionic radii were found to be between 137 and 154 pm[24], and an average of 145 pm could be estimated for hydrides. The sum of r_{VDW} of the protons and hydrides is 265 pm.
[22] A. Bondi, *J. Phys. Chem.* **1964**, *68*, 441–451.
[23] [23a] N. L. Allinger, J. A. Hirsch, M. A. Miller, I. J. Tyminski, F. A. Van Catledge, *J. Am. Chem. Soc.* **1968**, *90*, 1199–1210. – [23b] N. L. Allinger, Y. H. Yuh, J. H. Lii, *J. Am. Chem. Soc.* **1989**, *111*, 8551–8565; 8566–8575; 8576–8582.
[24] K. M. Mackay in *Comprehensive Inorganic Chemistry* (Eds.: J. C. Bailar, H. J. Emeléus, R. Nyholm, A. F. Trotman-Dickenson), Pergamon Press, New York, **1993**, vol. 1, p. 30.
[25] J. E. Huheey, E. A. Keiter, R. L. Keiter, *Inorganic Chemistry*, 4th ed., Harper Collins College Publishers, New York, **1993**, Table 8.1.
[26] H. Bock, K. Ruppert, C. Näther, Z. Haulas, H.-F. Herrmann, C. Arad, I. Göbel, A. John, J. Meuret, S. Nick, A. Rauschenbach, W. Seitz, T. Vaupel, and B. Solouki, *Angew. Chem.* **1992**, *104*, 564; *Angew. Chem. Int. Ed. Engl.* **1992**, *31*, 550–581.
[27] [27a] A. K. Abdul-Sada, A. M. Greenway, P. B. Hitchcock, T. J. Mohamed, K. R. Seddon, J. A. Zora, *J. Chem. Soc., Chem. Commun.* **1986**, 1753–1754. – [27b] A. J. Arduengo, III, S. F. Gamper, M. Tamm, J. C. Calabrese, F. Davidson, H. A. Craig, *J. Am. Chem. Soc.* **1995**, *117*, 572–573.
[28] K. Töpel, K. Hensen, J. W. Bats, *Acta Crystallogr., Sect. C*, **1984**, *40*, 828–830.
[29] [29a] K. Iijima, Y. Oonishi, S. Shibata, *Chem. Lett.* **1983**, 251–254. – [29b] K. Töpel, K. Hensen, M. Trömel, *Acta Crystallogr., Sect. B*, **1981**, *37*, 969–971.
[30] [30a] J. L. Hoard, S. Geller, W. M. Cashin, *Acta Crystallogr.* **1951**, *4*, 396–398. – [30b] D. Seebach, *Angew. Chem.* **1990**, *102*, 1363; *Angew. Chem. Int. Ed. Engl.* **1990**, *29*, 1320, Schemes 7 and 9.
[31] T. Schaefer, R. Sebastian, S. R. Salman, *Can. J. Chem.* **1981**, *59*, 3026–3029.
[32] V. Jonas, G. Frenking, *J. Chem. Soc., Chem. Commun.* **1984**, 1489–1490.
[33] C. W. Bird, G. W. H. Cheeseman in *Comprehensive Heterocyclic Chemistry* (Eds.: A. R. Katritzki, C. W. Rees), Pergamon Press, Oxford, **1984**, vol. 4, chapter 3.01, p. 29.
[34] [34a] M. Begtrup, R. M. Claramount, J. Elguero, *J. Chem. Soc., Perkin Trans 2*, **1978**, 99–104. – [34b] T. Bondgaard, H. J. Jakobsen, E. J. Rahkamaa, *J. Magn. Reson.* **1975**, *19*, 345–356.
[35] [35a] N. Platzer, J.-J. Basselier, P. Demerseman, *Bull. Soc. Chim. Fr.* **1974**, 905–912. – [35b] M. G. Reinecke, H. W. Johnson Jr., J. F. Sebastian, *J. Am. Chem. Soc.* **1969**, *91*, 3817–3823.
[36] [36a] F. Balkau, M. L. Heffernan, *Aust. J. Chem.* **1973**, *26*, 1501–1522. – [36b] A. Ahond, C. Poupat, P. Potier, *Tetrahedron* **1978**, *34*, 2385–2388. – [36c] J. Giraud, C. Marzin, *Org. Magn. Reson.* **1979**, *12*, 647–651.
[37] N. Farfán, R. Contreras, *J. Chem. Soc., Perkin Trans. 2*, **1987**, 771–773.
[38] I. I. Padilla-Martínez, A. Ariza-Castolo, R. Contreras, *Magn. Reson. Chem.* **1993**, *31*, 189–193.
[39] M. Hansen, H. J. Jakobsen, *J. Magn. Reson.* **1973**, *10*, 74–84.
[40] [40a] B. Wrackmeyer, *J. Organomet. Chem.* **1985**, *297*, 265–272. – [40b] M. Begtrup, J. Elguero, R. Faure, P. Camps, C. Estopá, D. Ilavský, A. Fruchier, C. Marzin, J. Mendoza, *Magn. Reson. Chem.* **1988**, *26*, 134–151.
[41] [41a] M. P. Williamson, D. H. Williams, *J. Am. Chem. Soc.* **1981**, *103*, 6580–6585. – [41b] Atta-ur-Rahaman, *One and Two Dimensional NMR Spectroscopy*, Elsevier, Amsterdam, **1989**, p. 167–197. – [41c] A. E. Derome, *Modern NMR Techniques for Chemistry Research*, Pergamon Press, Oxford, **1989**, p. 97–127. – [41d] D. Neuhaus, M. Williamson, *The Nuclear Overhauser Effect*, VCH, New York, **1989**, Figure 3.7.
[42] H. C. Brown, *Organic Synthesis via Boranes*, Wiley Interscience, New York, **1975**.

[95176]